



Published in final edited form as:

*Dalton Trans.* 2009 January 7; (1): 177–184. doi:10.1039/b808831d.

## Synthesis and characterization of the copper(II) complexes of new N<sub>2</sub>S<sub>2</sub>-donor macrocyclic ligands: synthesis and *in vivo* evaluation of the <sup>64</sup>Cu complexes†

Grazia Papini<sup>a</sup>, Simone Alidori<sup>a</sup>, Jason S. Lewis<sup>†,b,c</sup>, David E. Reichert<sup>b,c</sup>, Maura Pellei<sup>a</sup>, Giancarlo Gioia Lobbia<sup>a</sup>, Gráinne B. Biddlecombe<sup>b</sup>, Carolyn J. Anderson<sup>b,c</sup>, and Carlo Santini<sup>a</sup>

Jason S. Lewis: lewisj2@mskcc.org; Carlo Santini: carlo.santini@unicam.it

<sup>a</sup>Dipartimento di Scienze Chimiche, Università di Camerino, via S. Agostino 1, 62032, Camerino, MC, Italy

<sup>b</sup>Division of Radiological Sciences, Washington University School of Medicine, St. Louis, MO 63110, USA

<sup>c</sup>Alvin J. Siteman Cancer Center, Washington University School of Medicine, St. Louis, MO, 63110, USA

### Abstract

The aim of this work was to prepare a novel class of <sup>64</sup>Cu(II) labeled complexes with the new macrocyclic ligands 1,10-dithia-4,7-diazacyclododecane-3,8-dicarboxylic acid (NEC-SE, **1**), 1,10-dithia-4,7-diazacyclotridecane-3,8-dicarboxylic acid (NEC-SP, **2**) and 1,10-dithia-4,7-diazacyclotetradecane-3,8-dicarboxylic acid, (NEC-SB, **3**) to evaluate the usefulness of these macrocycles for potential utility as <sup>64</sup>Cu(II) chelators. The corresponding non-radioactive complexes [Cu(NEC-SE)]·3H<sub>2</sub>O (**4**), [Cu(NEC-SP)]·3H<sub>2</sub>O (**5**) and [Cu(NEC-SB)] (**6**) were prepared and their <sup>64</sup>Cu-analogs, [<sup>64</sup>Cu(NEC-SE)] (**7**) and [<sup>64</sup>Cu(NEC-SP)] (**8**) and [<sup>64</sup>Cu(NEC-SB)] (**9**) were produced in >98% radiochemical purity. Rats were injected with complex **7**, **8** or **9** and were euthanized at 1, 4 and 24 h. All three complexes are cleared from the blood over the first hour following injection but there is poor clearance of this activity over 24 h. A similar pattern of retention was noted in the liver where the levels of activity in this tissue at 1 h are not statistically different from those at 24 h. Molecular mechanics and DFT studies were performed on the complexes in order to gain insight into the lower stability.

†Electronic supplementary information (ESI) available: Complete biodistribution data (%ID/g and %ID/organ) for 19 harvested tissues at 1, 4 and 24 h for [<sup>64</sup>Cu(NEC-SE)] (**7**), [<sup>64</sup>Cu(NEC-SP)] (**8**) and [<sup>64</sup>Cu(NEC-SB)] (**9**) in male, Lewis rats. See DOI: 10.1039/b808831d

## Introduction

Copper radionuclides offer an attractive foundation for the development of disease-targeting radiopharmaceuticals; with a wide range of half-lives and decay schemes they have utility in both Positron Emission Tomography (PET) ( $^{60}\text{Cu}$ ,  $^{61}\text{Cu}$ ,  $^{62}\text{Cu}$  and  $^{64}\text{Cu}$ ) and targeted radiotherapy ( $^{64}\text{Cu}$  and  $^{67}\text{Cu}$ ).<sup>1,2</sup> Attachment of these nuclides to biomolecules, such as peptides and antibodies, require conjugation of the nuclide to the biological entity *via* a stable bifunctional ligand that can withstand metabolism and demetalation *in vivo*; the *in vivo* stability of the metal chelate is perhaps one of the most important considerations in the design of a disease-targeting copper radiopharmaceutical. The identification of kinetically inert radiocopper complexes, rather than copper complexes with high thermodynamic stability, is the first stage in identifying a suitable bifunctional chelator for copper nuclides.<sup>3,4</sup> Macrocyclic ligands form metal complexes which in general are thermodynamically more stable than complexes with analogous open-chain ligands and this has been termed the “macrocyclic effect”.<sup>3,5–12</sup> In addition macrocyclic metal complexes are often inert towards acid dissociation.<sup>13</sup> Due to the interest in macrocycles for use as bifunctional chelators, a large number of comparative studies on macrocycles with different donors and ring sizes have been recently published.<sup>14–16</sup> The majority of bifunctional ligands used for complexing copper have centered around the tetraaza-based macrocycles.<sup>16</sup> In general, studies have involved conjugation of 1,4,7,10-tetraazacyclododecane- $\text{N,N',N''N''''}$ -tetraacetic acid (DOTA) or 1,5,8,11-tetraazacyclotetradecane- $\text{N,N',N'',N''''}$ -tetraacetic acid (TETA) to the terminal amine of tumor-targeting peptides for subsequent labeling with  $^{64}\text{Cu}$  ( $t_{1/2} = 12.7$  h, 17.4%  $\beta^+$ , 41% EC, 40%  $\beta^-$ ,  $E_{\text{avg}} = 278$  keV) for PET imaging applications.<sup>17–21</sup> However, image quality is often less than optimal due to the slow release of uncoordinated  $^{64}\text{Cu}$  by decomposition of the complex in the blood or transchelation in the liver, causing elevated uptake in non-target tissues such as the liver.<sup>4,22</sup> New cross-bridged cyclam chelates (*e.g.*, CB-TE2A)<sup>4,23</sup> have recently been developed for  $^{64}\text{Cu}$  and have shown significant metal-chelate stability and as a consequence a lowering in non-target tissue accumulation.<sup>22,24</sup>

As mentioned, the dominant moieties for copper chelates have been the tetraaza-based ( $\text{N}_4$ ) macrocyclic ligands, with little or no studies done with  $\text{N}_2\text{S}_2$ -based macrocycles. Thiaazacycloalkanes exhibit interesting properties intermediate between those of cyclic polyamines and polythioethers.<sup>25</sup> The discovery of  $(\text{N}_2\text{S}_2)^{4-}$  donor sites in biology based on cysteine-X-cysteine tripeptide motifs has prompted the examination of small molecule models that build on a well known literature that is based on  $(\text{N}_2\text{S}_2)^{2-}$  ligands, which evolved over several decades.<sup>26,27</sup> Although *N,N*-ethylene-di-L-cysteine (EC) has been known for a long time,<sup>28</sup> it is surprising that macrocyclic ligands based on the EC skeletons have not been extensively investigated. EC copper(II),<sup>29</sup> nickel(II),<sup>30</sup> cobalt(III),<sup>31</sup>  $[\text{Tc}(\text{V})\text{O}]^{3+}$ ,<sup>32,33</sup>  $[\text{Re}(\text{V})\text{O}]^{3+}$ ,<sup>34–36</sup> molybdenum(VI),<sup>37</sup> indium(III) and gallium(III)<sup>38</sup> complexes have been synthesized and characterized. EC can be labeled with  $^{99\text{m}}\text{Tc}$  easily and efficiently with high radiochemical purity and stability.<sup>39–43</sup> Compared to metals with an oxidation state of +3 or higher, in the metal(II) complexes (copper(II) and nickel(II)) the EC acts as tetradentate  $\text{N}_2\text{S}_2$  ligand to form complexes with nearly planar *cis*- $\text{NiN}_2\text{S}_2$ <sup>30</sup> and *cis*- $\text{CuN}_2\text{S}_2$  units.<sup>29</sup> The bulky carboxylic or ester groups are equatorially oriented on the  $\lambda$

conformation NS chelate rings.<sup>44</sup> The *non*-macrocyclic N<sub>2</sub>S<sub>2</sub> moiety has been used as a means to attach radiocopper to biomolecules.<sup>45,46</sup> Siegfried and Kaden measured the rate of formation and dissociation of a series of N<sub>2</sub>S<sub>2</sub> macrocycles with Cu<sup>2+</sup> and Ni<sup>2+</sup>.<sup>15</sup> The ring size (from 12- to 16-membered cycles) and the geometry (*cis* or *trans*) of the arrangement of the donor groups was systematically varied in order to investigate how these two parameters affect the mechanism of complex formation and dissociation. In particular this study showed that the 14-membered macrocycle (*cis*-arrangement) forms complexes in which both Cu<sup>2+</sup> and Ni<sup>2+</sup> are ideally coordinated so that the dissociation becomes extremely slow.<sup>47–49</sup> The marked dependence of the nature of the backbone on the specificity of copper complexes of EC led us to investigate further EC-proligands with extended 12-, 13- and 14-member backbones as ligands for the development of new copper radiopharmaceuticals. It was hoped that these ligands would better accommodate both Cu(I) and Cu(II). A series of 12-, 14- and 16-membered N<sub>2</sub>S<sub>2</sub>-macrocycles and the related Cu(I) and Cu(II) derivatives were synthesized and their stabilities, redox and spectroscopic properties were explored.<sup>15,50–52</sup> In general it was shown that complexes with the smaller rings react as flexible open-chain ligands directly with H<sup>+</sup>, with the larger rings reacting in a similar manner as rigid ligands.<sup>15</sup> It was shown that the 14-membered macrocycle forms complexes in which the metal ions are ideally coordinated so that their dissociation becomes extremely slow. In view of a radiochemical application, N<sub>2</sub>S<sub>2</sub>-macrocycles with ring sizes varying between 12 and 16, as well as two 12-membered N<sub>2</sub>S<sub>2</sub>-rings with a pendant carboxylic and amino group linked to the N atoms, respectively, were also synthesized, and related Ag(I) complexes were tested in blood serum for their stability.<sup>53</sup>

In this current study we aimed to prepare three novel N<sub>2</sub>S<sub>2</sub> macrocyclic ligands based on the L,L-ethylenedicysteine skeletons. We present the synthesis and characterization of these novel ligands, the non-radioactive copper complexes and the corresponding <sup>64</sup>Cu-analogs. We further report the *in vivo* characteristics of these <sup>64</sup>Cu complexes in an animal model using acute biodistribution and we discuss the usefulness of these agents as bifunctional chelates for copper nuclides.

## Results

### Synthesis and characterization of the macrocyclic ligands

The reaction scheme of the syntheses of 1,10-dithia-4,7-diazacyclododecane-3,8-dicarboxylic acid (NEC-SE, **1**), 1,10-dithia-4,7-diazacyclotridecane-3,8-dicarboxylic acid (NEC-SP, **2**) and 1,10-dithia-4,7-diazacyclotetradecane-3,8-dicarboxylic acid, (NEC-SB, **3**) is shown in Fig. 1. The starting material ethylenedicysteine was prepared by the sodium reduction of the precursor L-thiazolidine-4-carboxylic acid in liquid ammonia according to methods described by Blondeau *et al.*<sup>32</sup> The ligands (**1**, **2** or **3**) were purified by washing with water and ethanol and were obtained in high yield. Their authenticity was confirmed by <sup>1</sup>H-NMR, <sup>13</sup>C-NMR, elemental analysis, IR and ESI-MS spectroscopy. The novel ligands **1** and **2** are white, the ligand **3** is yellow. They are microcrystalline solids, soluble in water solutions at pH > 7 and insoluble in common organic solvents; the ligand **3** is soluble in methanol solution. The infrared spectra of **1–3** showed broad absorptions in the range 3390–3412 cm<sup>-1</sup> due to the NH stretching vibrations. The presence of the COO moiety is

detected by intense, broad absorptions in the range 1586–1633  $\text{cm}^{-1}$ , due to the ionized  $\text{COO}^-$  stretching bands, and by medium or weak absorptions at 1726–1732  $\text{cm}^{-1}$ , attributable to the  $\text{COOH}$  un-ionized stretching frequencies. This behavior is in accordance with the coexistence of the predominant zwitterion together with a minority of the un-ionized carboxylic groups.<sup>54</sup> The formation of the macrocycle is confirmed by the presence of the  $\text{S}(\text{CH}_2)_n\text{S}$  protons in the  $^1\text{H-NMR}$  at  $\delta$  2.63–2.70 for **1**, at  $\delta$  1.72 and 2.49–2.77 for **2** and at  $\delta$  1.50 and 2.40–2.60 for **3**. In the  $^{13}\text{C}\{^1\text{H}\}$ NMR spectrum of **1** the chemical shifts of the  $\text{S-CH}_2$  carbons are observed at  $\delta$  34.74 and 37.21; for **2** the corresponding  $^{13}\text{C}$  chemical shifts of the  $\text{S-CH}_2$  carbons are at  $\delta$  33.56 and 37.07, while for **3** the  $^{13}\text{C}$  chemical shifts of the  $\text{S-CH}_2$  carbons are at  $\delta$  30.52 and 33.44. In addition, in **2**, the chemical shift of the  $\text{C-CH}_2\text{-C}$  carbon is at  $\delta$  31.48, while for **3** the corresponding  $^{13}\text{C}$  chemical shift of the  $\text{C-CH}_2\text{CH}_2\text{-C}$  carbons are at  $\delta$  27.11. The ESI-MS negative-ion spectrum of **1** in  $\text{H}_2\text{O}/\text{NH}_4\text{OH}$  is dominated by the deprotonated species  $[\text{M} - \text{H}]^-$  and  $[2\text{M} - \text{H}]^-$  at  $m/z$  293 (100%) and 588 (80%), respectively. The ESI-MS negative-ion spectrum of **2** in  $\text{H}_2\text{O}/\text{NH}_4\text{OH}$  is dominated by the deprotonated ligands  $[\text{M} - \text{H}]^-$  and  $[\text{M} - 2\text{H}]^{2-}$  at  $m/z$  307 (100%) and 153 (30%), respectively. The ESI-MS negative-ion spectrum of **3** in  $\text{H}_2\text{O}/\text{NH}_4\text{OH}$  is dominated by the deprotonated species  $[\text{M} - 2\text{H}]^{2-}$  at  $m/z$  160 (100%).

### Synthesis and characterization of the non-radioactive Cu(II) complexes

Ligands **1–3** were used in the preparation of the copper(II) complexes  $[\text{Cu}(\text{NEC-SE})]\cdot 3\text{H}_2\text{O}$  (**4**),  $[\text{Cu}(\text{NEC-SP})]\cdot 3\text{H}_2\text{O}$  (**5**), and  $[\text{Cu}(\text{NEC-SB})]$  (**6**); the chemical scheme of the syntheses of the compounds is given in Fig. 2. The stoichiometry of the compounds was not affected by either reducing or increasing the amount of the corresponding ligand. The blue copper complexes are insoluble in common organic solvents and not very soluble in water solutions at  $\text{pH} > 7$ . The authenticity of **4–6** was confirmed by elemental analysis and IR spectroscopy. The infrared spectra of the derivatives **4–6** showed broad absorptions in the range 3397–3412  $\text{cm}^{-1}$  due to the  $\text{NH}$  stretching vibrations. The presence of the  $\text{COO}$  moiety is detected by intense broad absorptions in the ranges 1601–1617  $\text{cm}^{-1}$  and 1358–1384  $\text{cm}^{-1}$ , due to the asymmetric and symmetric stretching modes, respectively; the shift to blue of the coordinated  $\text{COO}$  asymmetric stretchings with respect to the free ligands being observed upon complex formation. The observed range is in accordance with the values reported for coordinated  $\text{COO}$  stretching bands in amino-carboxylate metal complexes.<sup>54</sup> The magnitude of  $\nu_{\text{asymCOO}} - \nu_{\text{symCOO}}$  ( $\nu$ ) separation can be used to explain the type of carboxylate structure present in the solid state.  $\nu$  values for **4–6** are of about 250  $\text{cm}^{-1}$ , characteristic of monodentate coordination compounds. In the low-frequency region the copper–nitrogen stretching frequencies fall in the range 440–470  $\text{cm}^{-1}$ , while the copper–oxygen vibrations are detected in the range 300–380  $\text{cm}^{-1}$ .<sup>55</sup>

### Synthesis and characterization of the $^{64}\text{Cu}$ (II) complexes

The corresponding  $^{64}\text{Cu}$ -analogs,  $[\text{Cu}(\text{NEC-SE})]$  (**7**) and  $[\text{Cu}(\text{NEC-SP})]$  (**8**) and  $[\text{Cu}(\text{NEC-SB})]$  (**9**) were produced from reacting  $^{64}\text{CuCl}_2$  and either **1**, **2** or **3** in 0.1 M ammonium acetate buffer ( $\text{pH}$  8.0) at 90  $^\circ\text{C}$  for 1 h. It was necessary to dissolve **3** in 20  $\mu\text{L}$  methanol prior to diluting with the 0.1 M ammonium acetate buffer. The presence in solution of the  $^{64}\text{Cu}$ -complexes was confirmed by radio-TLC by comparison with the TLC

profile of an authentic sample of non-radioactive complex (**4**, **5** or **6**). The complexes were produced in a radiochemical purity of >98%. Compound **9** was additionally analyzed by radio-HPLC and was shown to have a radioactive peak at  $t_R = 12.61$  min, which corresponded to the UV peak for the analogous cold complex.

### *In vivo* data

The biodistribution data (percent injected dose per gram, %ID/g) of [ $^{64}\text{Cu}(\text{NEC-SE})$ ] (**7**) and [ $^{64}\text{Cu}(\text{NEC-SP})$ ] (**8**) and [ $^{64}\text{Cu}(\text{NEC-SB})$ ] (**9**) in male Lewis rats is summarized in Table 1. Fig. 3 presents a comparison between the biodistribution data (%ID/organ) of **7**, **8** and **9** and selected  $^{64}\text{Cu}$ -tetraazamacrocycles at 24 h post injection.<sup>56</sup> The data obtained from complexes **7**, **8** and **9** are indistinguishable. Although blood clearance of these complexes is observed over the first hour post injection (**7**,  $0.850 \pm 0.051$  %ID/g; **8**,  $0.820 \pm 0.046$  %ID/g; **9**,  $0.874 \pm 0.140$  %ID/g) the clearance from the blood was poor over 24 h (**7**,  $0.768 \pm 0.040$  %ID/g; **8**,  $0.774 \pm 0.031$  %ID/g; **9**,  $0.692 \pm 0.151$  %ID/g). The kidney did demonstrate partial clearance of the radioactivity over 24 h but still remained at relatively high levels. The liver and kidney uptakes of the complexes were high at 1 h post injection (liver: **7**,  $3.919 \pm 0.363$  %ID/g; **8**,  $3.151 \pm 0.286$  %ID/g; **9**,  $4.105 \pm 0.465$  %ID/g; kidney: **7**,  $8.662 \pm 0.551$  %ID/g; **8**,  $9.438 \pm 1.019$  %ID/g; **9**,  $8.895 \pm 0.612$  %ID/g), with little or no clearance observed for either complex from the liver over 24 h (liver: **7**,  $3.314 \pm 0.476$  %ID/g; **8**,  $3.182 \pm 0.188$  %ID/g; **9**,  $3.296 \pm 0.728$  %ID/g; kidney: **7**,  $4.906 \pm 0.211$  %ID/g; **8**,  $5.070 \pm 0.518$  %ID/g; **9**,  $4.738 \pm 0.617$  %ID/g). The poor clearance of these complexes suggests that the complexes are dissociating in tissues and  $^{64}\text{Cu}$  remains trapped in these tissues hindering clearance.<sup>57</sup>

### Discussion

In this current study we prepared three novel  $\text{N}_2\text{S}_2$  macrocyclic ligands 1,10-dithia-4,7-diazacyclododecane-3,8-dicarboxylic acid (NEC-SE, **1**), 1,10-dithia-4,7-diazacyclotridecane-3,8-dicarboxylic acid (NEC-SP, **2**), and 1,10-dithia-4,7-diazacyclotetradecane-3,8-dicarboxylic acid (NEC-SB, **3**) based on the L,L-ethylenedicycysteine skeleton. It is anticipated that the use of macrocyclic  $\text{N}_2\text{S}_2$  ligands would result in an increase in *in vivo* metal-chelate stability and therefore lead to an improvement in target to non-target tissue ratios. This has been demonstrated before and has been termed to “macrocycle-effect”.<sup>3,5-12</sup> We synthesized and characterized all the non-radioactive (**4-6**) and the  $^{64}\text{Cu}$  complexes (**7-9**) of these three ligands (Fig. 1 and 2). We further studied the *in vivo* biodistribution of complexes **7**, **8** and **9** in healthy rats to compare the biokinetics of these three compounds with previously reported data obtained with selected  $^{64}\text{Cu}$ -tetraazamacrocycles.

The biodistribution of complexes **7**, **8** and **9** were very similar to each other and very few statistical differences between the data exist. All three complexes were cleared from the blood over the first hour following injection but there was poor clearance of this activity over 24 h (Table 1). A similar pattern of retention is noted in the liver where the levels of activity in this tissue at 1 h are not statistically different from those at 24 h. The kidney did demonstrate partial clearance of the complexes over 24 h but still remained at relatively high

levels. The retention of activity in tissues was similar to that observed with  $^{64}\text{Cu}$ -cyclam<sup>29</sup> (Fig. 3) and  $^{64}\text{Cu}$ -monooxo-tetrazamacrocyclic complexes.<sup>4</sup> However, on comparison with  $^{64}\text{Cu}$ -TETA and  $^{64}\text{Cu}$ -DOTA, the uptake and retention of **7**, **8** and **9** are orders-of-magnitude higher (Fig. 3). This could in part be attributed to the kinetics of these hydrophilic complexes, but is more likely due to very rapid dissociation of the  $^{64}\text{Cu}$  from the chelates *in vivo*. This results in a biodistribution being more similar to “free”  $^{64}\text{Cu}$  than the biokinetics of intact  $\text{N}_2\text{S}_2$  complexes. This same dissociation phenomenon is observed (although slower) with  $\text{N}_4$ -macrocyclic chelates such as DOTA.  $^{64}\text{Cu}$  has been shown to dissociate *in vivo* from DOTA and DOTA-conjugates<sup>16</sup> and then undergoes metabolism and transchelation to superoxide dismutase and other proteins causing increased blood and liver accumulation.<sup>22,24</sup> The poor clearance of **7**, **8** and **9** suggests that the  $^{64}\text{Cu}$  complexes are rapidly degraded in blood and tissues and the  $^{64}\text{Cu}$  is sequestered by proteins and thereby remaining trapped in these tissues hindering clearance. The cross-bridged cyclam chelator, CBTE2A, has demonstrated improved *in vivo* stability and consequently a reduction in transchelation when compared to the non-bridged analog, TETA.<sup>4,16,22,24</sup> Conjugation of this chelate to tumor-targeting peptides has caused an improvement in non-target organ clearance and higher tumor ratios compared with either the  $^{64}\text{Cu}$ -TETA and  $^{64}\text{Cu}$ -DOTA analogs.<sup>16,24</sup>

In a recent report by Siegfried and Kaden, the kinetics of the formation and dissociation of  $\text{Cu}^{2+}$  from a series  $\text{N}_2\text{S}_2$  macrocycles was studied.<sup>15</sup> The ring size and the geometry of the arrangement of the donor groups were varied and the kinetic characteristics of the complexes were compared. Since all attempts to obtain crystal structures of the copper complexes were unsuccessful, molecular modeling was performed to gain insight into the geometries of the complexes that may be contributing to *in vivo* instability. The molecular modeling studies provide support for the role of the carboxylic acid groups in coordinating the copper atoms. The preferred structure for **7** is a square pyramidal complex with the base formed from one of the N atoms, two O atoms each donated by one of the carboxylate groups, and one of the S atoms. The apical position is filled by the remaining ring nitrogen, and the remaining ring S is 2.957 Å from the copper. The complex retains an essentially planar arrangement of the N and S atoms, planes defined by N–Cu–N and S–Cu–S intersect with a 27° angle comparable to the 21° found by Schugar.<sup>40</sup> Complex **8** prefers an octahedral coordination arrangement with the equatorial positions filled by the ring nitrogens and sulfurs, and the axial positions filled by carboxylate oxygens. The N and S atoms are even more planar than in **7** with the N–Cu–N and S–Cu–S planes separated by only 13.2°. Complex **9** was found to favor a distorted tetrahedral arrangement with the copper being coordinated by the carboxylates and both ring sulfurs. As with **8**, the N–Cu–N and S–Cu–S planes are separated by only 13.4°. The structures of these models are shown in Fig. 4, and a structural summary in Table 2.

The NBO analysis provides a method for analyzing the strength of the bonding interactions present in the complexes; an examination of the relative strengths for each donor–copper interaction provides a means to determine the predominate interactions for each complex. The copper center in complex **7** is strongly coordinated by one of the nitrogens (N12 242.62 kcal mol<sup>-1</sup>) and sulfur (S6 679.65 kcal mol<sup>-1</sup>) and oxygen (O17 246.44 kcal mol<sup>-1</sup>), while

the other nitrogen (N9 161.36 kcal mol<sup>-1</sup>) and oxygen (O19 173.08 kcal mol<sup>-1</sup>) display weaker interactions with the copper. Complex **8** is more balanced in terms of its bonding interactions, with both nitrogens (N10 and N14, 138.7 and 154.61 kcal mol<sup>-1</sup>) and sulfurs (S3 and S7, 370.61 and 375.46 kcal mol<sup>-1</sup>) having relatively equal interactions. In a similar trend both oxygen donors (O18 and O20) have respective bond strengths of 183.27 and 183.04 kcal mol<sup>-1</sup>. Complex **9** also shows relatively equivalent interaction strengths between pairs of donor atoms and the copper center, the two nitrogens (N11 and N14) have energies of 113.58 and 130.29 kcal mol<sup>-1</sup>, while the two sulfurs (S3 and S8) have energies of 351.91 and 376.49 kcal mol<sup>-1</sup>. The two oxygen donors also interact in an equivalent fashion (O19 and O21) 175.58 and 174.6 kcal mol<sup>-1</sup>.

The stability of these complexes therefore appear to be a balance of favorable donor–copper interactions and steric strain caused by their macrocyclic nature. In all cases the macrocycle is able to adopt a conformation in which the copper can sit in the plane of the ring, however the interactions between the donor atoms and copper vary greatly. All three systems contain three types of donor groups: nitrogen, sulfur, and oxygen; no one type of metal donor interaction seems strong enough to override the others. In complex **7** it appears that macrocyclic constraints prevent optimal overlap of the donor atoms with the copper center, most likely lowering the *in vivo* stability of the complex. Complexes **8** and **9** appear to be equally well coordinated with the available donor atoms, although it does appear that there may be less than maximal coordination with the sulfur donors when compared with the strength of the Cu–S6 bond found in complex **7**. This would suggest that the lower stability may arise from weaker Cu–S interactions than would be found in a non-macrocyclic ligand.

## Conclusions

We prepared three novel N<sub>2</sub>S<sub>2</sub> macrocyclic ligands NEC-SE (**1**), NEC-SP (**2**) and NEC-SB (**3**) based on the L,L-ethylenedicycysteine skeleton. From ligands **1**, **2** and **3** we have synthesized and characterized the non-radioactive copper complexes (**4–6**) and the analogous <sup>64</sup>Cu complexes (**7–9**). To the best of our knowledge, this is the first report of <sup>64</sup>Cu labeled to this form of (N<sub>2</sub>S<sub>2</sub>) macrocyclic ligand. It is however evident that the biological behavior of these complexes is less than ideal and additional study is required to improve the *in vivo* stability of these agents. In fact, the new ligands described in this manuscript are susceptible to further functionalization, for example by modification of the ring dimensions, and/or, by change of the donor atoms set.

## Experimental

### Methods and materials

**Chemicals and analysis**—All syntheses and handling were carried out under an atmosphere of dry oxygen-free dinitrogen, using standard Schlenk techniques or a glove box. All solvents were dried, degassed and distilled prior to use. Elemental analyses (C, H, N, S) were performed in house with a Fisons Instruments 1108 CHNS-O Elemental Analyser. Melting points were taken on an SMP3 Stuart Scientific Instrument. IR spectra were recorded as neat from 4000 to 600 cm<sup>-1</sup> with a Perkin-Elmer Spectrum One System and as Nujol mulls from 600 to 100 cm<sup>-1</sup> with a Perkin-Elmer System 2000 FT-IR

instrument. IR annotations used: m = medium, mbr = medium broad, s = strong, sbr = strong broad, sh = shoulder, w = weak.  $^1\text{H}$ - and  $^{13}\text{C}$ -NMR spectra were recorded on a Oxford-400 Varian spectrometer (400.4 MHz for  $^1\text{H}$ , 100.1 MHz for  $^{13}\text{C}$ ). Chemical shifts ( $\delta$ ) are quoted relative to internal  $\text{SiMe}_4$ . NMR annotations used: br = broad, m = multiplet, qn = quintet, t = triplet. Electrospray mass spectra (ESI-MS) were obtained in positive- or negative-ion mode on a Series 1100 MSD detector HP spectrometer, using an acetone mobile phase. The compounds were added to reagent grade methanol to give solutions of approximate concentration 0.1 mM. These solutions were injected (1  $\mu\text{L}$ ) into the spectrometer *via* a HPLC HP 1090 Series II fitted with an autosampler. The pump delivered the solutions to the mass spectrometer source at a flow rate of 300  $\mu\text{L min}^{-1}$ , and nitrogen was employed both as a drying and nebulizing gas. Capillary voltages were typically 4000 V and 3500 V for the positive- and negative-ion mode, respectively. Confirmation of all major species in this ESI-MS study was aided by comparison of the observed and predicted isotope distribution patterns, the latter calculated using the IsoPro 3.0 computer program.

**Radiochemistry**—All chemicals unless otherwise stated were purchased from Sigma-Aldrich Chemical Co. (St. Louis, MO). Water was distilled and then deionized (18 M $\Omega$   $\text{cm}^{-2}$ ) by passing through a Milli-Q water filtration system (Millipore Corp., Milford, MA). Radioactivity was counted with a Beckman Gamma 8000 counter containing a NaI crystal (Beckman Instruments, Inc., Irvine, CA). Care was taken to ensure all buffers and vials were as free of metal contaminants as possible. The non-radioactive copper complexes (**4**, **5** and **6**) were used as fully characterised non-radioactive standards to confirm the identity of the  $^{64}\text{Cu}$  analogs (**7**, **8** and **9**). Identification of the  $^{64}\text{Cu}$  complexes was performed using radio thin-layer chromatography (radio-TLC). Radio-TLC detection was accomplished using a BIOSCAN AR2000 Imaging Scanner (Washington, DC). TLC was performed using glass-backed silica gel and a 10% aqueous  $(\text{CH}_3\text{COO})\text{NH}_4$  solution : methanol (1 : 1) as mobile phase. Reaction progress and purity were also monitored by analytical reversed-phase HPLC, which was performed on a Waters 600E (Milford, MA) chromatography system with a Waters 991 photodiode array detector and an Ortec Model 661 radioactivity detector (EG & G Instruments, Oak Ridge, TN). A Vydak C-18 column was employed with a gradient that changes from 0.1% TFA in water to 5 : 95 0.1% TFA in Water : 0.1 % TFA in  $\text{CH}_3\text{CN}$  over the course of 25 min. Unreacted  $^{64}\text{Cu}$  was eluted in the void volume,  $t_{\text{R}} < 1.0$  min.

### Ligand synthesis and characterization

**Synthesis of 1,10-dithia-4,7-diazacyclododecane-3,8-dicarboxylic acid (NEC-SE, **1**)**—Ethylenedicysteine was synthesised according to literature methods.<sup>26</sup>

Ethylenedicysteine (5.50 g, 20.50 mmol) and 1,2-dibromoethane (3.85 g, 20.50 mmol) were added to 100 mL of a  $\text{NaHCO}_3$  solution (6.89 g, 82.01 mmol). The mixture was gradually heated up to 100  $^\circ\text{C}$  and was stirred for 24 h to obtain a clear pale yellow solution. The solution was cooled to room temperature and acidified to pH 2. The resulting precipitate which separated out was filtered and washed with water ( $3 \times 50$  mL) and ethanol ( $3 \times 15$  mL) and dried under reduced pressure to yield derivative **1** in 65% yield. Melting point, 225–228  $^\circ\text{C}$ .  $^1\text{H}$  NMR ( $\text{D}_2\text{O}/\text{NaOD}$ , 293 K):  $\delta$  2.49 (br, 4H,  $\text{CH}_2\text{N}$ ), 2.63–2.70 (m, 8H,  $\text{CH}_2\text{S}$ ), 3.10 (t, 2H,  $\text{CH}$ ).  $^{13}\text{C}\{^1\text{H}\}$  NMR ( $\text{D}_2\text{O}/\text{NaOD}$ , 293 K):  $\delta$  34.74, 37.21 ( $\text{CH}_2\text{S}$ ), 49.26 ( $\text{CH}_2\text{N}$ ), 65.75 ( $\text{CH}$ ), 182.81 ( $\text{CO}_2\text{H}$ ). IR ( $\text{cm}^{-1}$ ): 3390br ( $\nu\text{NH}$ ), 1730sh



( $\nu_{\text{asym}}\text{COOH}$ ), 1586s ( $\nu_{\text{asym}}\text{COO}^-$ ), 610br, 532s, 459m, 399w, 376sbr, 267w, 255w. ESI-MS (major negative-ions,  $\text{H}_2\text{O}/\text{NH}_4\text{OH}$ ),  $m/z$  (%): 293 (100)  $[\text{M} - \text{H}]^-$ , 588 (60)  $[2\text{M} - \text{H}]^-$ . Anal. Calcd. for  $\text{C}_{10}\text{H}_{18}\text{N}_2\text{O}_4\text{S}_2$ : C, 40.80; H, 6.16; N, 9.52; S, 21.78%. Found: C, 41.05; H, 6.26; N, 9.37; S, 21.53%.

**Synthesis of 1,10-dithia-4,7-diazacyclotridecane-3,8-dicarboxylic acid (NEC-SP, 2)**—The ligand NEC-SP, **2**, was prepared analogously to **1**. Ethylenedicycysteine (5.50 g, 20.50 mmol) and 1,3-dibromopropane (4.14 g, 20.50 mmol) were added to a  $\text{NaHCO}_3$  (6.89 g, 82.01 mmol) solution (100 mL). The mixture was gradually heated up to 100 °C and stirred for 24 h to obtain a clear yellow solution. The solution was cooled to room temperature and acidified to pH 2. The precipitate which separated out was filtered, washed with water ( $3 \times 50$  mL) and ethanol ( $3 \times 25$  mL) and dried under reduced pressure to yield derivative **2** in 72% yield. Melting point, 212–215 °C.  $^1\text{H}$  NMR ( $\text{D}_2\text{O}/\text{NaOD}$ , 293 K):  $\delta$  1.72 (qn, 2H,  $\text{CH}_2$ ), 2.54 (br, 4H,  $\text{CH}_2\text{N}$ ), 2.61–2.77 (m, 8H,  $\text{CH}_2\text{S}$ ), 3.22 (t, 2H, CH),  $^{13}\text{C}\{^1\text{H}\}$  NMR ( $\text{D}_2\text{O}/\text{NaOD}$ , 293 K):  $\delta$  31.48 ( $\text{CH}_2$ ), 33.56 ( $\text{CH}_2\text{S}$ ), 37.07 ( $\text{CH}_2\text{S}$ ), 48.57 ( $\text{CH}_2\text{N}$ ), 65.55 (CH), 181.68 ( $\text{CO}_2\text{H}$ ). IR ( $\text{cm}^{-1}$ ): 3412br ( $\nu\text{NH}$ ), 1732m ( $\nu_{\text{asym}}\text{COOH}$ ), 1588s ( $\nu_{\text{asym}}\text{COO}^-$ ), 633w, 573w, 536sbr, 439m, 373s, 279w. ESI-MS (major negative-ions,  $\text{H}_2\text{O}/\text{NH}_4\text{OH}$ ),  $m/z$  (%): 153 (30)  $[\text{M} - 2\text{H}]^{2-}$ , 307 (100)  $[\text{M} - \text{H}]^-$ . Anal. Calcd. for  $\text{C}_{11}\text{H}_{20}\text{N}_2\text{O}_4\text{S}_2$ : C, 42.84; H, 6.54; N, 9.08; S, 20.79%. Found: C, 42.75; H, 6.61; N, 8.97; S, 20.33%.

**Synthesis of 1,10-dithia-4,7-diazacyclotetradecane-3,8-dicarboxylic acid, (NEC-SB, 3)**—Ethylenedicycysteine (5.50 g, 20.50 mmol) was added to a methanol/water (4 : 1) solution (100 mL) of NaOH (3.28 g, 82.01 mmol) and the solution was stirred at room temperature for 2 h. 1,4-dibromobutane (4.43 g, 20.50 mmol) were added and the mixture was stirred for 48 h to obtain a clear yellow solution. The solution was acidified to pH 2. The precipitate which separated out was filtered, washed with water ( $3 \times 50$  mL) and ethanol ( $2 \times 25$  mL) and dried under reduced pressure to yield derivative **3** in 70% yield. Melting point, 202 °C (decomposition).  $^1\text{H}$  NMR ( $\text{D}_2\text{O}/\text{NaOD}$ , 293 K):  $\delta$  1.50 (br, 4H,  $\text{CH}_2$ ), 2.54 (br, 4H,  $\text{CH}_2\text{N}$ ), 2.64 (m, 8H,  $\text{CH}_2\text{S}$ ), 3.02 (t, 2H, CH).  $^{13}\text{C}\{^1\text{H}\}$  NMR ( $\text{D}_2\text{O}/\text{NaOD}$ , 293 K):  $\delta$  27.11 ( $\text{CH}_2$ ), 30.52 ( $\text{CH}_2\text{S}$ ), 33.44 ( $\text{CH}_2\text{S}$ ), 45.73 ( $\text{CH}_2\text{N}$ ), 61.90 (CH), 179.46 ( $\text{CO}_2\text{H}$ ). IR ( $\text{cm}^{-1}$ ): 3397br ( $\nu\text{NH}$ ), 1726m ( $\nu_{\text{asym}}\text{COOH}$ ), 1633s ( $\nu_{\text{asym}}\text{COO}^-$ ), 634w, 616w, 569m, 552m, 536m, 457w, 376w, 280m. ESI-MS (major negative-ions,  $\text{H}_2\text{O}/\text{NH}_4\text{OH}$ ),  $m/z$  (%): 160 (100)  $[\text{M} - 2\text{H}]^{2-}$ . Anal. Calcd. for  $\text{C}_{12}\text{H}_{22}\text{N}_2\text{O}_4\text{S}_2$ : C, 44.70; H, 6.88; N, 8.69; S, 19.89%. Found: C, 44.55; H, 6.72; N, 8.38; S, 19.44%.

### Complex synthesis and characterization

**Synthesis of  $[\text{Cu}(\text{NEC-SE})] \cdot 3\text{H}_2\text{O}$  (**4**)**—Complex **4** was prepared by stirring **1** (0.293 g, 1.0 mmol) and  $(\text{CH}_3\text{COO})_2\text{Cu}$  (0.200 g, 1.0 mmol) in 30 mL of  $\text{H}_2\text{O}$  for 6 h at room temperature. The resulting blue solid was filtered off, washed with water ( $3 \times 50$  mL) and ethanol ( $3 \times 25$  mL) and dried under reduced pressure to yield **4** in 85% yield. Melting point, 179–182 °C (decomposition). IR ( $\text{cm}^{-1}$ ): 3409br ( $\nu\text{NH}$ ), 3210w ( $\nu\text{OH}$ ), 1610 s ( $\nu_{\text{asym}}\text{COO}$ ), 1362 s ( $\nu_{\text{sym}}\text{COO}$ ), 644mbr, 556br, 528br, 467br, 430w, 400w, 377m, 337m, 310br. Anal. Calcd. for  $\text{C}_{10}\text{H}_{22}\text{CuN}_2\text{O}_7\text{S}_2$ : C, 29.30; H, 5.41; N, 6.83; S, 15.64%. Found: C, 29.41; H, 5.48; N, 6.60; S, 15.46%.

**Synthesis of [Cu(NEC-SP)]·3H<sub>2</sub>O (5)**—Complex **5** was prepared by stirring **2** (0.308 g, 1.0 mmol) and (CH<sub>3</sub>COO)<sub>2</sub>Cu (0.200 g, 1.0 mmol) in 30 mL of H<sub>2</sub>O at room temperature for 6 h. The resulting blue precipitate was filtered off, washed with water (3 × 50 mL) and ethanol (3 × 25 mL) and dried under reduced pressure to yield **5** in 77% yield. Melting point, 173–176 °C (decomposition). IR (cm<sup>-1</sup>): 3412br (νNH), 3162wbr (νOH), 1617s (ν<sub>asym</sub>COO), 1384s (ν<sub>sym</sub>COO), 640br, 460 m, 445sh, 377w, 350br, 268w, 255w. Anal. Calcd. for C<sub>11</sub>H<sub>24</sub>CuN<sub>2</sub>O<sub>7</sub>S<sub>2</sub>: C, 31.16; H, 5.71; N, 6.61; S, 15.12%. Found: C, 31.11; H, 5.58; N, 6.41; S, 14.97%.

**Synthesis of [Cu(NEC-SB)] (6)**—Complex **6** was prepared by stirring **3** (0.322 g, 1.0 mmol) and (CH<sub>3</sub>COO)<sub>2</sub>Cu (0.200 g, 1.0 mmol) in 30 mL of H<sub>2</sub>O at room temperature for 6 h. The resulting blue precipitate was filtered off, washed with water (3 × 50 mL) and ethanol (3 × 25 mL) and dried under reduced pressure to yield **6** in 67% yield. Melting point, 187 °C (decomposition). IR (cm<sup>-1</sup>): 3397br (νNH), 3209br (νOH), 1601s (ν<sub>asym</sub>COO), 1358s (ν<sub>sym</sub>COO), 617m, 592w, 568w, 553br, 400br, 385br, 330br, 301w, 280m. Anal. Calcd. for C<sub>12</sub>H<sub>20</sub>CuN<sub>2</sub>O<sub>4</sub>S<sub>2</sub>: C, 37.54; H, 5.25; N, 7.30; S, 16.70%. Found: C, 37.35; H, 5.07; N, 7.19; S, 16.53%.

**Synthesis of radiocomplexes [<sup>64</sup>Cu(NEC-SE)] (7), [<sup>64</sup>Cu(NEC-SP)] (8) and [<sup>64</sup>Cu(NEC-SB)] (9)**—Copper-64 was produced and purified as previously described.<sup>58</sup> <sup>64</sup>CuCl<sub>2</sub> (200 μCi) was diluted in 100 μL of 0.1 M ammonium acetate buffer (pH 7.5). 0.25 mg of **1**, **2**, or **3** was dissolved in 100 μL of the same buffer, and then added to the <sup>64</sup>Cu solution. It was necessary to dissolve **3** in 20 μL methanol prior to diluting with the 0.1 M ammonium acetate buffer. After vigorous stirring of the resulting mixture at 90 °C for 1 h, deprotonation and coordination of the enantiomerically pure macrocycle to the metal center occurred. The presence in solution of the labeled complexes was established by TLC (**7**, R<sub>f</sub> = 0.32; **8**, R<sub>f</sub> = 0.35; **9**, R<sub>f</sub> = 0.55) by comparison with the TLC profile of an authentic sample of the corresponding non-radioactive complex. The complexes were produced in a radiochemical purity of >98%. For the biodistribution studies the radioactive complexes were diluted with 0.9% saline.

### Biodistribution studies

All animal experiments were conducted in compliance with the Guidelines for the Care and Use of Research Animals established by Washington University's Animal Studies Committee. Male Lewis rats (30-day old, Charles River Laboratories, Inc., Wilmington, MA) were injected with either complex **7**, **8** or **9** (~40 μCi in 150 μL). Rats were examined at 3 time points (n = 4 per group at 1, 4 and 24 h). In all studies following euthanasia, 19 tissues and organs of interest were removed and weighed, and the radioactivity present was measured in a γ-counter. The percent dose per gram (%ID/g) and percent dose per organ (%ID/organ) were then calculated on comparison to known standards.

### Molecular modeling

All three copper complexes were studied utilizing a three-step approach. First each copper complex was built by hand and geometry optimized in the program PCModel<sup>59</sup>, using the GMX force field.<sup>60</sup> This is a MM2-like valence force field and uses a Urey-Bradley force

field about metal centers. Monte Carlo based conformational searches, GMMX, similar to that developed by Saunders *et al*<sup>61</sup> were performed on each complex in order to optimize the geometry about the copper atoms. The lowest energy conformation of each complex was then exported to the program AMPAC<sup>62</sup> and optimized using the SAM/1D Hamiltonian. The optimized structures were then exported into JAGUAR and DFT calculations (B3LYP/LACVP\*) were then performed on each complex followed by a NBO analysis.<sup>63</sup>

## Supplementary Material

Refer to Web version on PubMed Central for supplementary material.

## Acknowledgments

We are very grateful for the technical assistance of Christopher Sherman. Thanks also to Tom Voller and the WUSTL cyclotron facility staff for radionuclide production. This work was partially supported by grants from the National Institutes of Health/National Cancer Institute (NIH/NCI) (CA86307 and CA93375), by University of Camerino (FAR 2007), and by Ministero dell'Istruzione dell'Università e della Ricerca (PRIN 2007).

## Abbreviations

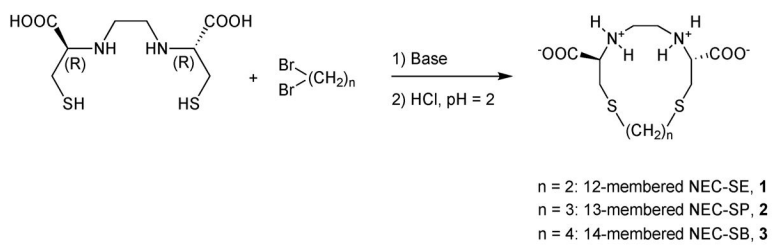
<b>DOTA</b>	1,4,7,10-Tetraazacyclododecane-N,N',N'',N'''-tetraacetic acid
<b>EC</b>	N,N-Ethylene-di-L-cysteine
<b>NMR</b>	Nuclear magnetic resonance
<b>ESI-MS</b>	Electrospray ionization mass spectroscopy
<b>IR</b>	Infra-red
<b>NEC-SE</b>	1,10-Dithia-4,7-diazacyclododecane-3,8-dicarboxylic acid
<b>NEC-SP</b>	1,10-Dithia-4,7-diazacyclotridecane-3,8-dicarboxylic acid
<b>NEC-SB</b>	1,10-Dithia-4,7-diazacyclotetradecane-3,8-dicarboxylic acid
<b>PET</b>	Positron emission tomography
<b>TETA</b>	1,5,8,11-Tetraazacyclotetradecane-N,N',N'',N'''-tetraacetic acid
<b>TLC</b>	Thin layer chromatography

## Notes and references

- Blower PJ, Lewis JS, Zweit J. Nucl Med Biol. 1996; 23:957–980. [PubMed: 9004284]
- McQuade P, Rowland DJ, Lewis JS, Welch MJ. Curr Med Chem. 2005; 12:807–818. [PubMed: 15853713]
- Moi MK, Meares CF, McCall MJ, Cole WC, DeNardo SJ. Anal Biochem. 1985; 148:249–253. [PubMed: 4037304]
- Sun X, Wuest M, Weisman GR, Wong EH, Reed DP, Boswell CA, Motekaitis R, Martell AE, Welch MJ, Anderson CJ. J Med Chem. 2002; 45:469–477. [PubMed: 11784151]
- Anderson CJ, Welch MJ. Chem Rev. 1999; 99:2219–2234. [PubMed: 11749480]
- Cabbiness DK, Margerum DW. J Am Chem Soc. 1969; 91:6540–6541.
- Heeg MJ, Jurisson SS. Acc Chem Res. 1999; 32:1053–1060.
- Hubin TJ. Coord Chem Rev. 2003; 241:27–46.

9. Kaden TA. Dalton Trans. 2006:3617–3623. [PubMed: 16865171]
10. Li M, Meares CF, Zhong GR, Miers L, Xiong CY, DeNardo SJ. Bioconjugate Chem. 1994; 5:101–104.
11. Liu S, Edwards DS. Bioconjugate Chem. 2001; 12:7–34.
12. Meyer M, Dahaoui-Gindrey V, Lecomte C, Guillard RC. Coord Chem Rev. 1998; 178–180:1313–1405.
13. Izatt RM, Bradshaw JS, Nielsen SA, Lamb JD, Christensen JJ, Sen D. Chem Rev. 1985; 85:271–339.
14. Delgado R, Félix V, Lima LMP, Price DW. Dalton Trans. 2007:2734–2745. [PubMed: 17592589]
15. Siegfried L, Kaden TA. Dalton Trans. 2005:1136–1140. [PubMed: 15739018]
16. Wadas TJ, Wong EH, Weisman GR, Anderson CJ. Curr Pharm Des. 2007; 13:3–16. [PubMed: 17266585]
17. Anderson CJ, Dehdashti F, Cutler PD, Schwarz SW, Laforest R, Bass LA, Lewis JS, McCarthy DW. J Nucl Med. 2001; 42:213–221. [PubMed: 11216519]
18. Anderson CJ, Jones LA, Bass LA, Sherman ELC, McCarthy DW, Cutler PD, Lanahan MV, Cristel ME, Lewis JS, Schwarz SW. J Nucl Med. 1998; 39:1944–1951. [PubMed: 9829587]
19. Lewis JS, Lewis MR, Cutler PD, Srinivasan A, Schmidt MA, Schwarz SW, Morris MM, Miller JP, Anderson CJ. Clin Cancer Res. 1999; 5:3608–3616. [PubMed: 10589778]
20. Lewis JS, Lewis MR, Srinivasan A, Schmidt MA, Wang J, Anderson CJ. J Med Chem. 1999; 42:1341–1347. [PubMed: 10212119]
21. McQuade P, Miao Y, Yoo J, Quinn TP, Welch MJ, Lewis JS. J Med Chem. 2005; 48:2985–2992. [PubMed: 15828837]
22. Boswell CA, Sun X, Niu W, Weisman GR, Wong EH, Rheingold AL, Anderson CJ. J Med Chem. 2004; 47:1465–1474. [PubMed: 14998334]
23. Wong EH, Weisman GR, Hill DC, Reed DP, Rogers ME, Condon JS, Fagan MA, Calabrese JC, Lam KC, Guzei IA, Rheingold AL. J Am Chem Soc. 2000; 122:10561–10572.
24. Spraugue JE, Peng Y, Sun X, Weisman GR, Wong EH, Achilefu S, Anderson CJ. Clin Cancer Res. 2004; 10:8674–8682. [PubMed: 15623652]
25. Westerby BC, Juntunen KL, Leggett GH, Pett VB, Koenigbauer MJ, Purgett MD, Taschner MJ, Ochrymowycz LA, Rorabacher DB. Inorg Chem. 1991; 30:2109–2120.
26. Bouwman E, Driessen WL, Reedijk J. Coord Chem Rev. 1990; 104:143–172.
27. Busch DH, Jicha DC. Inorg Chem. 1:884–887.
28. Crooks, HM. The Chemistry of Penicillin. Princeton University Press; Princeton, NJ: 1949.
29. Bharadwaj PK, Potenza JA, Schugar HJ. J Am Chem Soc. 1986; 108:1351–1352.
30. Stibrany RT, Fox S, Bharadwaj PK, Schugar HJ, Potenza JA. Inorg Chem. 2005; 44:8234–8242. [PubMed: 16270960]
31. Okamoto K, Fushimi N, Konno T, Hidaka J. Bull Chem Soc Jpn. 1991; 64:2635–2643.
32. Blondeau P, Berse C, Gravel D. Can J Chem. 1967; 45:49–52.
33. Davison A, Jones AG, Orvig C, Sohn M. Inorg Chem. 1981; 20:1629–1632.
34. Hansen L, Lipowska M, Taylor A, Marzilli LG. Inorg Chem. 1995; 34:3579–3580.
35. Hansen L, Hirota S, Xu X, Taylor AT, Marzilli LG. Inorg Chem. 2000; 39:5731–5740. [PubMed: 11151373]
36. Hansen L, To Yue K, Xu X, Lipowska M, Taylor A, Marzilli LG. J Am Chem Soc. 1997; 119:8965–8972.
37. Berg JM, Spira DJ, Hodgson KO, Bruce AE, Miller KF, Corbin JL, Stiefel EI. Inorg Chem. 1984:23.
38. Anderson CJ, John CS, Li YJ, Hancock RD, McCarthy TJ, Martell AE, Welch MJ. Nucl Med Biol. 1995; 22:165–173. [PubMed: 7767309]
39. Van Nerom CG, Bormans GM, De Roo MJ, Verbruggen AM. Eur J Nucl Med. 1993; 20:738–746. [PubMed: 8223766]
40. Verbruggen AM, Nosco DL, Van Nerom CG, Bormans GM, Adriaens PJ, De Roo MJ. J Nucl Med. 1992; 33:551–557. [PubMed: 1532419]

41. Yang DJ, Azhdarinia A, Wu P, Yu DF, Tansey W, Kalimi SK, Kim EE, Podoloff DA. *Cancer Biotherapy Radiopharm.* 2001; 16:73–83.
42. Zareneyrizi F, Yang DJ, Oh CS, Ilgan S, Yu DF, Tansey W, Liu CW, Kim EE, Podoloff DA. *Anti-Cancer Drugs.* 1999; 10:685–692. [PubMed: 10507319]
43. Yang DJ, Ilgan S, Higuchi T, Zareneyrizi F, Oh CS, Liu CW, Kim EE, Podoloff DA. *Pharm Res.* 1999; 16:743–750. [PubMed: 10350019]
44. Buchanan I, Minelli M, Ashby MT, King TJ, Enemark JH, GCD. *Inorg Chem.* 1984; 23:495–500.
45. Anderson CJ, Rocque PA, Weinheimer CJ, Welch MJ. *Nucl Med Biol.* 1993; 20:461–467. [PubMed: 8504288]
46. Fujibayashi Y, Matsumoto K, Arano Y, Yonekura Y, Konishi J, Yokoyama A. *Chem Pharm Bull Tokyo.* 1990; 38:1946–1948. [PubMed: 2268894]
47. Rorabacher DB. *Inorg Chem.* 1966; 5:1891–1899.
48. Taylor RW, Stepien HK, Rorabacher DB. *Inorg Chem.* 1974; 13:1282–1289.
49. Turan TS, Rorabacher DB. *Inorg Chem.* 1972; 11:288–295.
50. Siegfried L, Kaden TA. *Helv Chim Acta.* 1984; 67:29–38.
51. Balakrishnan KP, Kaden TA, Siegfried L, Züberbuhler AD. *Helv Chim Acta.* 1984; 67:1060–1069.
52. Kaden TA, Kaderli S, Sager W, Siegfried-Hertli LC, Züberbuhler AD. *Helv Chim Acta.* 1986; 69:1216–1223.
53. Riesen PC, Kaden TA. *Helv Chim Acta.* 1995; 78:1325–1333.
54. Nakamoto, K. *Applications in Coordination, Organometallic, and Bioinorganic.* John Wiley & Sons, Inc; New York: 1997. p. 62-73.
55. Herlinger AW, Wenhold SL, Long TV II. *J Am Chem Soc.* 1970; 4:6474–6481.
56. Jones-Wilson TM, Deal KA, Anderson CJ, McCarthy DW, Kovacs Z, Motekaitis RJ, Sherry AD, Martell AE, Welch MJ. *Nucl Med Biol.* 1998; 25:523–530. [PubMed: 9751418]
57. Bass LA, Wang M, Welch MJ, Anderson CJ. *Bioconjugate Chem.* 2000; 11:527–532.
58. McCarthy DW, Shefer RE, Klinkowstein RE, Bass LA, Margeneau WH, Cutler CS, Anderson CJ, Welch MJ. *Nucl Med Biol.* 1997; 24:35–43. [PubMed: 9080473]
59. PCModel. Serena Software; Bloomington, IN: 2003.
60. Gajewski JJ, Gilbert KE, Kreek TW. *J Comput Chem.* 1997; 19:1167–1178.
61. Saunders M, Houk KN, Wu YD, Still WC, Lipton M, Chang G, Guida WC. *J Am Chem Soc.* 1990; 112:1419–1427.
62. AMPAC. Semichem, Inc; Shawnee Mission: 2004.
63. Glendenning, ED.; Badenhop, JK.; Reed, AE.; Carpenter, JE.; Bohman, JA.; Morales, CM.; Weinhold, F. NBO 5.0. Theoretical Chemistry Institute, University of Wisconsin; Madison, WI: 2001.

**Fig. 1.**

The reaction schemes of the syntheses of 1,10-dithia-4,7-diazacyclododecane-3,8-dicarboxylic acid (NEC-SE, **1**), 1,10-dithia-4,7-diazacyclotridecane-3,8-dicarboxylic acid (NEC-SP, **2**) and 1,10-dithia-4,7-diazacyclotetradecane-3,8-dicarboxylic acid, (NEC-SB, **3**).

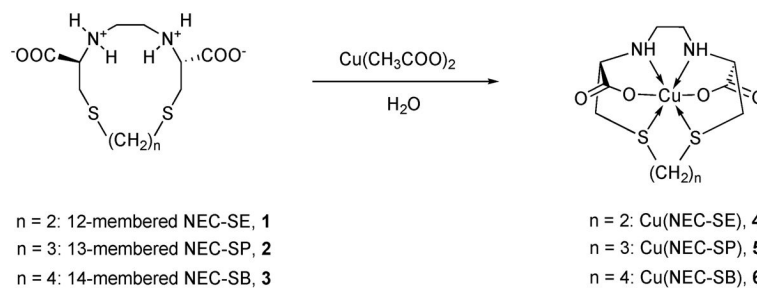


**Fig. 2.**  
The reaction schemes of the syntheses of Cu(NEC-SE) (**4**), Cu(NEC-SP) (**5**) and Cu(NEC-SB) (**6**).

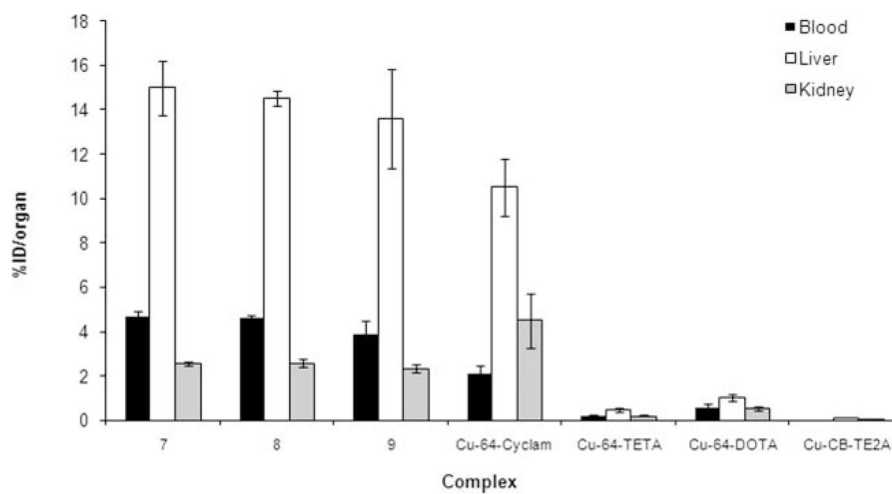


**Fig. 3.** Comparison between the biodistribution data (%ID/organ) of [ $^{64}\text{Cu}(\text{NEC-SE})$ ] (**7**), [ $^{64}\text{Cu}(\text{NEC-SP})$ ] (**8**) and [ $^{64}\text{Cu}(\text{NEC-SB})$ ] (**9**) and selected  $^{64}\text{Cu}$ -tetraazamacrocycles at 24 h post injection. Data for **7**, **8** and **9** obtained in male Lewis Rats.  $^{64}\text{Cu}$ -Cyclam,  $^{64}\text{Cu}$ -TETA,  $^{64}\text{Cu}$ -DOTA and  $^{64}\text{Cu}$ -CB-TE2A obtained in female Sprague-Dawley rats.<sup>4,56</sup>



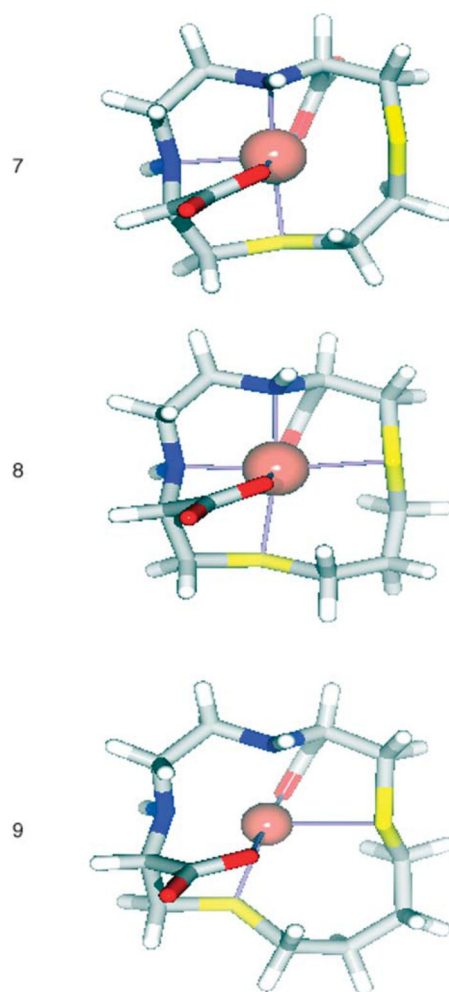


**Fig. 4.** The DFT (B3LYP/LACVP\*) optimized structures of Cu(NEC-SE) (**7**), Cu(NEC-SP) (**8**) and Cu(NEC-SB) (**9**).

Table 1

Biodistribution (percent dose per gram, %ID/g) of [<sup>64</sup>Cu(NEC-SE)] (7), [<sup>64</sup>Cu(NEC-SP)] (8) and [<sup>64</sup>Cu(NEC-SB)] (9) in male Lewis rats. Rats were injected with ~40 μCi of complex and were euthanized at 3 time points (n = 4 per group at 1, 4 and 24 h). Following euthanasia, 19 tissues and organs of interest were removed and weighed and the radioactivity present was measured in a γ-counter. Given are the %ID/g values for selected organs. The complete biodistribution data for all 19 tissues, including percent dose per organ (%ID/organ) values, can be found in the ESI<sup>†</sup>

Tissue	[ <sup>64</sup> Cu(NEC-SE)] (7), %ID/g			[ <sup>64</sup> Cu(NEC-SP)] (8), %ID/g			[ <sup>64</sup> Cu(NEC-SB)] (9), %ID/g		
	1 h	4 h	24 h	1 h	4 h	24 h	1 h	4 h	24 h
Blood	0.850 ± 0.051	0.897 ± 0.080	0.768 ± 0.040	0.820 ± 0.046	0.835 ± 0.021	0.774 ± 0.031	0.874 ± 0.140	0.879 ± 0.112	0.692 ± 0.151
Lung	0.838 ± 0.065	0.768 ± 0.045	0.723 ± 0.036	0.776 ± 0.089	0.737 ± 0.009	0.771 ± 0.061	1.673 ± 0.225	0.949 ± 0.109	0.746 ± 0.143
Liver	3.919 ± 0.363	3.905 ± 0.540	3.314 ± 0.476	3.151 ± 0.286	3.418 ± 0.371	3.182 ± 0.188	4.105 ± 0.465	3.866 ± 0.635	3.296 ± 0.728
Spleen	0.560 ± 0.025	0.731 ± 0.174	1.046 ± 0.106	0.483 ± 0.054	0.704 ± 0.014	1.078 ± 0.099	0.698 ± 0.168	0.815 ± 0.137	0.924 ± 0.207
Kidney	8.662 ± 0.551	7.849 ± 1.099	4.906 ± 0.211	9.438 ± 1.019	7.818 ± 0.663	5.070 ± 0.518	8.895 ± 0.612	7.096 ± 1.059	4.738 ± 0.617
Muscle	0.380 ± 0.032	0.344 ± 0.012	0.309 ± 0.026	0.393 ± 0.055	0.352 ± 0.017	0.319 ± 0.031	0.411 ± 0.056	0.330 ± 0.050	0.302 ± 0.033
Fat	0.334 ± 0.054	0.266 ± 0.068	0.163 ± 0.026	0.318 ± 0.074	0.214 ± 0.024	0.153 ± 0.019	0.371 ± 0.073	0.218 ± 0.037	0.136 ± 0.035
Heart	0.672 ± 0.086	0.774 ± 0.096	1.041 ± 0.070	0.657 ± 0.025	0.736 ± 0.048	1.013 ± 0.078	0.839 ± 0.228	0.752 ± 0.059	0.923 ± 0.189
Bone	1.131 ± 0.072	1.274 ± 0.082	0.984 ± 0.076	1.099 ± 0.098	1.255 ± 0.040	0.999 ± 0.065	1.143 ± 0.195	1.155 ± 0.161	0.855 ± 0.188

<sup>†</sup>Electronic supplementary information (ESI) available: Complete biodistribution data (%ID/g and %ID/organ) for 19 harvested tissues at 1, 4 and 24 h for [<sup>64</sup>Cu(NEC-SE)] (7), [<sup>64</sup>Cu(NEC-SP)] (8) and [<sup>64</sup>Cu(NEC-SB)] (9) in male, Lewis rats. See DOI: 10.1039/b808831d

Table 2

Structural features of B3LYP optimized complexes

Complex 7		Complex 8		Complex 9	
Cu-L (Å)		Cu-L (Å)		Cu-L (Å)	
N9	2.193	N10	2.154	N11	2.213
N12	1.997	N13	2.150	N14	2.188
S3	2.957	S3	2.553	S3	2.565
S6	2.341	S7	2.550	S8	2.540
O17	1.948	O18	1.967	O19	1.953
O19	2.053	O20	1.968	O21	1.955
Angle (°)		Angle (°)		Angle (°)	
N-Cu-N	91.94	N-Cu-N	88.21	N-Cu-N	84.66
S-Cu-S	98.77	S-Cu-S	103.55	S-Cu-S	112.21
O-Cu-N	86.02, 79.03	O-Cu-N	81.73, 81.49	O-Cu-N	81.62, 81.05